To flock or not to flock: The pros and cons of flocking in long-range "migration" of mobile robot swarms

Fatih Gökçe
KOVAN Research Lab.
Dept. of Computer Eng.
Middle East Technical Univ.
Ankara, Turkey
fgokce@ceng.metu.edu.tr

Erol Şahin
KOVAN Research Lab.
Dept. of Computer Eng.
Middle East Technical Univ.
Ankara, Turkey
erol@ceng.metu.edu.tr

ABSTRACT

This study investigates the pros and cons of flocking in long-range "migration" of mobile robot swarms under the influence of different factors. We present a flocking behavior consisting of three simple behaviors: heading alignment, proximal control, and alignment to the desired homing direction. The behavior drives a flock of robots from one location to another by sensing the magnetic field of the Earth. We propose that four factors influence the accuracy of reaching a particular location with the proposed behavior; namely, averaging through the heading alignment behavior, the noise in sensing the homing direction, the differences in the characteristics of the individuals, and the disturbances caused by proximal control behavior. In a series of systematic experiments conducted with both physical and simulated robots, we evaluate the effects of these factors in the accuracy of long-range "migrations" of flocks.

Categories and Subject Descriptors

I.2.9 [**Artificial Intelligence**]: Robotics

General Terms

Algorithms, Performance, Design, Experimentation

Keywords

swarm robotics, flocking, migration

1. INTRODUCTION

Every year, certain animal and insect species flock together to make long-range migrations to reach their feeding or breeding grounds. Migration is an impressive phenomenon because of its three important properties: (1) Very long distances scaling up to several thousands of kilometers are travelled. (2) Migratory animals and insects typically migrate in flocks (which may include millions) rather than as individuals. (3) Migration occurs in an accurate way despite different environmental conditions and hazards.

Biological studies indicated that these animals mainly use the magnetic field of the Earth [1, 21] (among various environmental cues [12, 14, 21]) to determine the direction of their travel. Among other aspects of the migration behavior, the accuracy of the flocks to reach the very same feeding or breeding grounds has attracted much interest. In [3], Bergman and Donner first suggested that the flock migration "increases the accuracy of orientation mechanism" which is known as the *many wrongs principle*. They suggested that flocking suppresses the tendencies of the individuals to migrate in slightly different directions. Hence the flock can align to an average direction of the preferences of the individuals giving a more accurate direction when compared to the case of individuals.

Hamilton [8] and Wallraff [20] reiterated the many wrongs principle in their theoretical studies. Hamilton [8] suggested that "the orientation of groups of animals is more accurate than that of individuals". Assuming that (1) the spatial goal is the same for all individuals, (2) the inaccuracies are represented by the deviation of individuals from the goal and (3) the individuals adopt their orientation to the mean direction of the individuals in the flock, he drew a series of theoretical curves with respect to flock size showing that average deviation from the goal decreases with the flock size. Wallraff [20] suggested some methods to analyze the observational data to investigate the effect of flocking to the accuracy of orientation toward the goal direction and described their statistical implications.

In [13], Rabøl et al. observed skylark flocks of different sizes (1, 2, 3-5, and 6 or more) on their spring migration. They showed that the dispersion of migratory directions becomes less scattered with the size of flock. Later, Tamm [17] observed similar results by testing the hypothesis on homing pigeons with three to six flocks. By selecting flocks in a random fashion, he showed that the flocks are more accurate than individuals and their homing time is shorter than that of individuals. However, some contradictory observations were also reported. In [10], Keeton compared mean bearings of single pigeons with that of flocks of four pigeons. He reported no significant difference between single birds and flocks in terms of accuracy. In [2], Benvenuti et al. compared the orientation behavior of single birds with that of small flocks ranging from three to ten birds. Their results showed that small flocks do not orient more accurately than single birds. In [6], Guilford et al. released pairs of homing pigeons in which none, one or both of the birds had previously been trained. They investigated whether unexperienced birds exploit the knowledge of other bird to achieve a navigational advantage or not. They found that unexperienced birds do

Cite as: To Flock or not to Flock: The Pros and Cons Of Flocking in Long-Range "Migration" of Mobile Robot Swarms, Fatih Gökçe, Erol Şahin, *Proc. of 8th Int. Conf. on Autonomous Agents and Multiagent Systems (AAMAS 2009),* Decker, Sichman, Sierra and Castelfranchi (eds.), May, 10–15, 2009, Budapest, Hungary, pp. 65–72

not prefer to home together with their pairs.

Recently, Simons has brought the almost forgotten many wrongs principle to light as a null model and general framework for testing the advantage of group navigation empirically [16]. Taking the principle in its simplest form in which there are no characteristic differences between individuals and contribution of individuals to the direction of flock are equal, he showed that large group size increases the accuracy of group navigation. He emphasized that the principle can be generalized to more complex scenarios in which there are differences between individuals and the individuals contribute to flock direction in an unequal manner.

The work of Simons has rejuvenated attention to the many wrongs principle. Codling et al. studied the principle in a scenario resembling to the migration of animals [4]. They developed a point-mass movement model incorporating a biased random walk behavior and the group interactions. They investigated the effect of navigational error, group size, interaction radius size and environmental turbulence to the performance of the behavior to navigate a group from one location to another. They found out that, with the exception of the high environmental turbulence case, the group movement provides a navigational advantage.

In robotics, Gutiérrez et al. [7] proposed a fully-distributed strategy for the improvement of odometry in collective robotics. In this strategy, the robots improve their estimate of location by exploiting the estimations of their neighbors. The estimate of each robot is associated with a confidence level decreasing with the distance travelled by the corresponding robot. Each robot combines its own estimate and the received estimates of its neighbors using the confidence level of each estimate to get a more precise location information. They evaluated their strategy in simulations on a foraging task in which the duty of the robots was to bring items from a resource site to a central place. Their results showed that as the group size increases both the quality of the individuals' estimates and the performance of the group improve.

As reviewed above, the interest in the role of flocking in long-range migrations has produced a number of hypotheses and models in biological systems. Despite the results obtained in simulations, coupled with few, sometimes contradictory observational data from animal flocks, the problem begs a constructivist approach.

In this paper, we investigate the effects of flocking in long-range travels using a swarm of physical and simulated mobile robots. Specifically, we extend a self-organized flocking behavior that was developed in our prior studies [18, 19] to enable the long-range "migration" of a robotic swarm by sensing the magnetic field of the Earth. Here, we use the term "long-range migration" in a simplistic way. We study how a swarm of robots, starting from a fixed point in space, would flock by following a certain pre-defined direction sensed through the magnetic field of the Earth for a pre-defined amount of time. In this sense, the guiding of the flock towards an arbitrary "breeding location" in space is beyond the scope of this work. Similarly, we exclude other strategies that are also known to be used in animals, such as the use of landmarks, from our study.

2. EXPERIMENTAL PLATFORM

We used the Kobot mobile robot (Figure 1(a)) and its physics-based simulator [18] as our experimental platform.

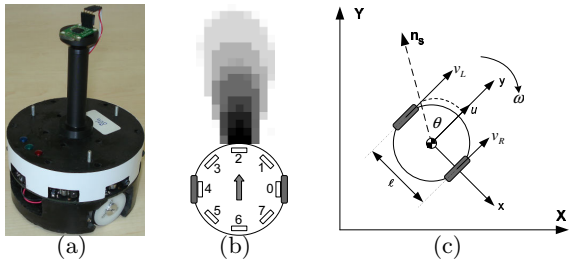

(a) (b) (c)

Figure 1: (a) The Kobot robot platform. (b) The scaled drawing of Kobot illustrating the circular body, wheels, placement of the sensors and range for 2^{nd} sensor. The sensors are placed uniformly at 45° intervals. Each square patch in the gray scale blob indicates the output of the sensor. (c) The body-fixed reference frame of robot is depicted. It is fixed to the center of the robot. The x-axis of the body-fixed reference frame coincides with the rotation axis of the wheels. The forward velocity (u) is along with the y-axis of the body-fixed reference frame. The angular velocity of the robot is denoted with ω. v_R and v_L are the velocities of the right and left motors, respectively. θ, current heading or the robot, is the angle between the y-axis of the body-fixed reference frame and the *sensed North* direction (n_s). l is the distance between the wheels.

2.1 Kobot mobile robot platform

Kobot is a CD-sized, differentially driven and power efficient platform weighing only 350 gr with batteries. It has 8 infrared (IR) sensors capable of kin and obstacle detection and a digital compass. The communication among robots as well as between the robots and a console is carried out through an IEEE 802.15.4/ZigBee compliant wireless communication module.

The *infrared short-range sensing system* (IRSS) measures the range and bearing of kin-robots and other objects in close proximity. It consists of eight infrared (IR) sensors placed uniformly at 45° intervals, as shown in Figure 1(b) and a coordinator microcontroller that controls the sensors. Each sensor is capable of measuring distances up to 20 cm at seven discrete levels and distinguishing robots from obstacles/walls at a rate of 18 Hz. The system used frequency modulated IR signals in range measurement and is shown to be immune to changes in environmental lighting conditions.

The output of k^{th} sensor is an integer pair (r_k, o_k). $r_k \in \{0, 1\}$ shows whether the detected object is a kin-robot or not. $o_k \in \{0, 1, \cdots, 7\}$ denotes the distance from the object being sensed. $o_k = 1$ and $o_k = 7$ indicate a distant and a nearby object, respectively. $o_k = 0$ stands for no detection.

The compass and the communication module of the robots are used to create the *virtual heading sensor* (VHS), which lets the robots to sense the relative headings of their neighbors. At each control step which is approximately 110 ms, a robot measures its own heading (θ) and then broadcasts it to the robots within the communication range. The heading measurement is done in clockwise direction with respect to the *sensed North* as shown in Figure 1(c). The neighbors whose heading values are received in a control step are called as VHS neighbors.

The heading value received from the j^{th} VHS neighbor (θ_{rj}) is converted to the body-fixed reference frame of the robot as[1]:

$$\theta_j = \theta - \theta_{rj} + \frac{\pi}{2}$$

where θ_j is the heading of the j^{th} VHS neighbor with respect to the body-fixed reference frame of the robot.

It is important to point out that the VHS does not assume the sensing of the absolute North direction and hence does not rely on the sensing of a global coordinate frame. Instead, the only assumption that VHS makes is that the *sensed North* remains approximately the same among the robots that are being communicated. As a matter of fact, in indoor environments ferrous metals are abundant and cause large deviations in the sensing of the magnetic field.

2.2 Simulator

The simulator is implemented using the Open Dynamics Engine physics-engine library [2]. The body and the wheels of the robot are modeled as cylinders and collision of the bodies and slippage in wheels are simulated. The actuation and sensing characteristics of Kobot are obtained from systematic experiments [18]. The IRSS is modelled based on samples collected in real robot experiments performed to characterize the proximal sensing and kin-detection capabilities of the robot. The VHS is modelled using the experiments conducted with Prowler [15], an event-driven probabilistic wireless network simulator, to characterize the effect of the wireless communication range (R) to the number of VHS neighbors (N_c). Based on these experiments, the range of wireless communication and the maximum number of VHS neighbors are set to to 20 m and 20 respectively. In a previous study [18], we verified that the results obtained from simulations were similar to the ones obtained from Kobots.

3. THE FLOCKING BEHAVIOR

Flocking in a group of simulated agents has attracted much interest from a wide range of fields ranging from computer graphics (for producing realistic animations) to control theory and statistical physics (see [18] for a review). However, the behaviors developed within these studies relied on unrealistic sensing and actuation abilities that do not exist on physical robots. Hence, the prior studies to our work reported in [18], such as [11, 9], have failed to generate self-organized flocking in a group of autonomous robots.

In this study, we extend the flocking behavior proposed in [18]. The original behavior consisted of heading alignment and proximal control components and is shown to drive the flock to wander aimlessly within an environment, avoiding obstacles on its path, with no preferred direction. In this study, we included a homing component to the original behavior and combine the three components in a weighted vector sum:

$$\vec{a} = \frac{\vec{h} + \beta \ \vec{p} + \gamma \ \vec{g}}{\|\vec{h} + \beta \ \vec{p} + \gamma \ \vec{g}\|}$$

where $\vec{h}$ is the heading alignment vector, $\vec{p}$ and $\vec{g}$ are the proximal control and homing direction alignment vectors with weights β and γ respectively. $\vec{a}$ is the desired heading vector for the robot that is normalized by Euclidean norm shown as $\| \cdot \|$.

3.1 Heading Alignment Behavior

The aim of the heading alignment behavior is to align the robot with the average heading of its neighbors. Using the the headings received from the VHS neighbors, the heading alignment vector ($\vec{h}$) is calculated as:

$$\vec{h} = \frac{\sum_{j \in \mathcal{N}_R} e^{i\theta_j}}{\| \sum_{j \in \mathcal{N}_R} e^{i\theta_j} \|}$$

where $\mathcal{N}_R$ denotes the set of VHS neighbors, when the communication range of VHS is set to R. θ_j is the heading of the j^{th} neighbor in the body-fixed reference frame.

3.2 Proximal Control Behavior

The proximal control behavior aims to maintain the cohesion of the flock while avoiding the obstacles. Using the data obtained from IRSS, the normalized proximal control vector, $\vec{p}$, is calculated as:

$$\vec{p} = \frac{1}{8} \sum_{k=1}^{8} f_k e^{i\phi_k}$$

where k refers to the sensor placed at angle $\phi_k = \frac{\pi}{4}k$ with the x-axis of the body-fixed reference frame (Figure 1(c)). f_k is the virtual force applied by k^{th} sensor to the robot which is calculated as:

$$f_k = \begin{cases} -\frac{(o_k - o_{des})^2}{C} & \text{if } o_k \geq o_{des} \\ \frac{(o_k - o_{des})^2}{C} & \text{otherwise} \end{cases}$$

where C is a scaling constant. o_k indicates the detection level for k^{th} sensor, namely the distance from the object. o_{des} is the desired detection level taken as 3 for kin-robots, and 0 for obstacles.

3.3 Homing behavior

The homing behavior aims to align the robot with the desired homing direction (θ_d). The homing direction alignment vector $\vec{g}$ is calculated as:

$$\vec{g} = \vec{g_d} - \vec{a_c}$$

where $\vec{g_d}$ is the desired homing direction vector in the body-fixed reference frame and $\vec{a}_c$ is the current heading vector of the robot coincident with the y-axis of the body-fixed reference frame.

In this paper, we assume that the desired homing direction is a constant that is provided to all the robots apriori. The starting point of the flock is fixed and initially all robots are aligned to homing direction. The duration of the travel is predetermined and no landmarks are used. With these assumptions, the behavior can be said to "migrate" a flock of

[1]The heading of the robot, θ is the angle between the *sensed North* and the y-axis of its body-fixed reference frame in clockwise direction, see Figure 1(c). $\frac{\pi}{2}$ is added to $\theta - \theta_{rj}$ to obtain the heading of the j^{th} neighbor in the body-fixed reference frame.

[2]URL:http://ode.org

robots to a particular "breeding location" and is only a partial model of long-range animal migration. Since landmarks are used and the goal direction may change during the travel in animal migration, our behavior should be considered to model a part of animal migration in which a long distance is travelled while the goal direction is fixed. It should be noted that the homing behavior only modulates the orientation of the robot and does not provide a criteria as to whether a homing position is reached or not.

3.4 Motion control

The forward (u) and angular (ω) velocities are calculated using the desired heading vector ($\vec{a}$). The forward velocity (u) is calculated as:

$$u = \begin{cases} (\vec{a} \cdot \vec{a}_c)\ u_{max} & \text{if } \vec{a} \cdot \vec{a}_c \geq 0 \\ 0 & \text{otherwise} \end{cases}$$

The dot product of the desired ($\vec{a}$) and current heading ($\vec{a}_c$) vectors is used to modulate the forward velocity of the robot. When the robot is moving in the desired direction, the dot product results in 1 and the robot attains its maximum forward velocity (u_{max}). If the robot deviates from the desired direction, the dot product and hence u decreases and converges to 0 when the angle between the two vectors gets closer to 90°. If the angle exceeds 90°, then the dot product is negative. In this case, u is set to 0 and the robot makes only rotation.

The angular velocity (ω) of the robot is controlled by a proportional controller using the angular difference between the desired and current heading vectors:

$$\omega = (\angle\vec{a}_c - \angle\vec{a})K_p$$

where K_p is the proportional gain of the controller.

The rotational speeds of the right and left motors (Figure 1(c)) are eventually calculated as follows:

$$N_R = \left(u - \frac{\omega}{2}l\right)\frac{60}{2\pi r}$$

$$N_L = \left(u + \frac{\omega}{2}l\right)\frac{60}{2\pi r}$$

where N_R and N_L are the rotational speeds (rotations per minute) of the right and left motors, respectively, l is the distance between the wheels of the robot (meters), u is the forward velocity (meters per second) and ω is the angular velocity (radians per second).

In this study, we used a default set of parameters (listed in Table 1) which are shown to generate stable flocking in both physical robots and simulations [18].

4. EXPERIMENTAL FRAMEWORK

The experiments with physical and simulated robots are conducted in an open environment with approximately constant magnetic field. Specifically, the robots operated in an environment, in which the walls and the obstacles remained beyond their proximal sensing ranges during the course of the experiments. Initially, the robots are placed on a hexagonal grid with a default center spacing of 25 cm and aligned to the desired homing direction which is fixed to a pre-defined value as illustrated in Figure 2. The center of each flock is always fixed at the same initial point. The features specific to the experimental setups of physical robots and simulations are described below.

Table 1: Default parameters for the behavior.

Parameter	Default Value
weight of proximal control (β)	12
weight of goal direction (γ)	4
proportional gain for angular velocity (K_p)	0.5
maximum forward speed (u_{max})	0.07 m/s
desired detection level (o_{des})	3

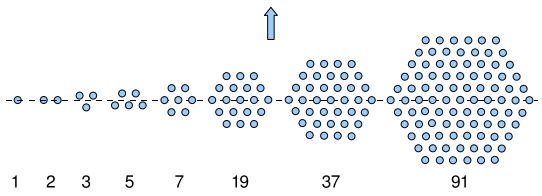

Figure 2: The topology of the robots for different flock sizes. The arrow indicates the homing direction.

4.1 Physical robots

We use flocks including up to 7 Kobots in an arena of size 4 × 12 m. The magnetic field in the arena, as shown in Figure 3, is not uniform and deviates approximately 6-degrees to left, between the starting and finishing lines of the course.

In each experiment, the robots are left to move from a particular starting point and the locations of the flock centers as the flock passes the finishing line are recorded.

4.2 Simulator

The experiments are conducted with flocks that include up to 91 simulated robots and executed for 1558 control steps which corresponds to approximately 171.38 seconds of simulated time. This duration is determined from a reference experiment in which a flock of 7 simulated robots traverses 12 m in an ideal world. A uniform magnetic field (without any deviation) is used in simulations. When we need to disable the proximal control behavior in simulations, we increase the center spacing to 20 m to hypothetically disable the effect of proximal control behavior. In this case, the range of wireless communication is also increased to 1600 m with the same scale up as in inter-robot spacing.

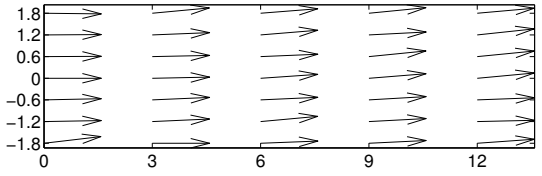

Figure 3: The magnetic field measured in the experiment arena. The field is tilted to the left approximately 6-degrees. The units of the axes are in meters.

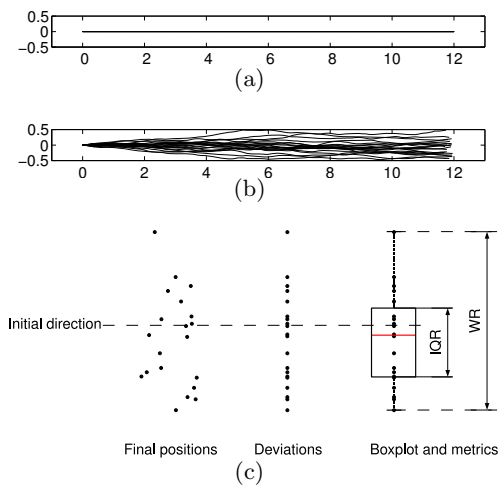

Figure 4: (a) In an ideal world, the robots migrate with perfect accuracy. The units of the axes are in meters and [0,0] is the starting point in (a) and (b). (b) The paths followed by the center of a flock in an environment with noise. Note that, the experiments are carried out in open environments and that the borders of the plots in (a) and (b) do *not* indicate the existence of walls. (c) Final positions, deviations of final positions from the initial direction, box-plot of the distribution of the deviations and IQR & WR are illustrated.

4.3 Metrics

We propose two metrics to evaluate the accuracy and efficiency of long-range migration. The first metric consists of inter-quartile and whisker ranges to evaluate the accuracy of migration along homing direction. The second metric is the average speed to evaluate the efficiency of the flocks.

4.3.1 Inter-quartile and whisker ranges

In an ideal world, free of noise and other external disturbances, the robots starting from a fixed place would always reach the exact same "breeding location" at all times with perfect accuracy (Figure 4(a)). However, in physical systems (whether they are robots or biological organisms), factors such as sensor noise would cause deviations at final positions reached at the end of the migration and hence the accuracy decreases. Therefore, the accuracy of a flock in migrating along a homing direction is directly related to the amount of scatter of the paths followed by the flock in different runs.

In order to measure the amount of scatter of the paths, we utilize some parameters obtained from a box-plot plotted using the deviations of the flock centers from initial direction at the final positions. For example in Figure 4(c), the final positions are depicted for the paths given in Figure 4(b). The distribution of deviations are shown in Figure 4(c). The box-plot of the distribution of these deviations is plotted on the right side of Figure 4(c). In this box-plot, the ends of the boxes and the horizontal line in between correspond to the first and third quartiles and the median values, respectively. The top and bottom whiskers indicate the largest and smallest non-outlier data, respectively. The data in between the first and third quartiles lie within the 50% confidence interval, while the data in between the whiskers lie within the 99.3% confidence interval. The distance between first and third quartiles is called as inter-quartile range (IQR) and the distance between the whiskers is referred as whisker range (WR). We use IQR & WR to quantify the amount of scatter. Lower values of IQR & WR indicate a more accurate path.

Note that, we are interested in the amount of scatter, and that the median (or the mean) of the final positions are not of interest. We prefer to use IQR and WR as our metrics instead of variance due to their relative robustness against outlier data.

4.3.2 Average speed

We use average speed (V_a) of flocks calculated by dividing total displacement of a flock to the time of operation as a measure of the efficiency of the movement. A high average speed is a sign of efficient movement driving the flock smoothly whereas a low average speed indicates inefficient and jerky motion. Note that, the parameters of the flocking can usually guarantee the cohesion of the flock.

5. FACTORS THAT INFLUENCE LONG-RANGE MIGRATION OF FLOCKS

We hypothesize that the following four factors influence the variance in the final positions.

Averaging through heading alignment (HA): The heading alignment behavior aims to align the individuals to the average heading of their neighbors. This is likely to allow the individuals to suppress the noise causing deviations in their headings and improve the accuracy of their alignment. The dynamics captured here can be considered to correspond to the many wrongs principle.

Noise in sensing the homing direction (HD): The homing direction, typically obtained from the Earth's magnetic field, can be considered to have noise. This noise can be caused by the characteristics of the sensor as well as external fluctuations in the magnetic field.

The noise in sensing the homing direction is modelled in simulator using the vectorial noise model [5] as:

$$\theta_d = \angle\{e^{i\theta'_d} + \eta_S e^{i\xi_S}\}$$

where θ'_d represents the actual homing direction, η_S is a parameter determining the magnitude of noise vector and ξ_S is the direction of the noise chosen from a Gaussian distribution $N(\mu = \theta'_d, \sigma = \pm\frac{\pi}{2})$ where μ and σ are the mean and standard deviation, respectively. The standard deviation of the resultant distribution is controlled by the value of η_S.

Finally, we would like to note that, the noise generated by the hard-iron effects depends much on the environment and is too complex, if not impossible, to model. In this sense, the noise model proposed here is very crude. However despite this, the results obtained in simulation and in Kobots can be matched qualitatively by choosing a large enough η_S value.

Differences in the characteristics of individuals (CD): Not all individuals in a flock are identical. For example, the birds in a migratory flock have different wing lengths, weights, et-cetera. Similarly, even the robots that are manufactured from the same components using the same process, tend to have slightly different sensor/actuator characteristics, as will be evaluated later.

Table 2: Investigated factors in the experiments.

Exp	HA	HD	CD	PD	Platform
1	+	-	-	+	Simulator
2	+	+	-	-	Simulator
3	+	+	+	+	Sim. & Phy. robots

In the simulator, we implement the individual differences as a bias term added to the right motor speed as:

$$N_R = N'_R + \xi_m \quad (1)$$

where N'_R is the actual speed of the right motor and ξ_m is the bias term in rotations per minute (rpm). ξ_m is chosen from a Gaussian distribution $N(\mu = \mu_i, \sigma)$. σ is fixed for all robots as 0.05 rpm, whereas, μ_i, the mean value for the i_{th} robot, is chosen from a Gaussian distribution $N(\mu = 0, \sigma = \pm 0.05)$.

This bias gives the robot a tendency to deviate towards left or right instead of moving straight. The direction of the tendency depends on the sign of μ_i.

Disturbances caused by proximal control behavior (PD): During flocking, the proximal control behavior aims to keep the flock cohesive yet make sure that no collisions happen among the individuals. This creates disturbances on the heading direction of the individuals.

These disturbances are implicit in the proximal sensing through the noise in the IRSS system and need not to be explicitly included.

6. EXPERIMENTS

In the experiments, we introduce one or more factors to the flocking behavior and investigate their effects on the accuracy of migration. Specifically, the factors included in each experiment set are presented in Table 2. Since the heading alignment is crucial for flocking, it is enabled in all experiments without noise.

In the first set of the experiments, we investigate the effect of disturbances caused by only proximal control. In the second set, we evaluate the effect of noise in sensing the homing direction alone. In the last set, the effect of individual differences is analyzed while proximal control is enabled and noise in sensing the homing direction is also present.

The first two sets of the experiments are carried out only in the simulator whereas the last set is conducted using both simulated and physical robots. Unless otherwise stated, the experiments are repeated for 500 and 5 times with simulated and physical robots, respectively to derive statistically significant results.

6.1 Effect of proximal disturbance

The proximal control behavior aims to avoid collisions with robots and obstacles and to maintain the cohesion of the flock using the sensory readings obtained from IRSS. Since IRSS has a noisy characteristic, the movement of the robots is disturbed due to false readings. Therefore, the accuracy of the flock in moving along the homing direction is affected.

In order to understand the effect of disturbances caused by the proximal control behavior, we leave only IRSS as a source of noise in the system and conduct experiments with flocks of different sizes. IQR & WR and average speeds are plotted in Figure 5(a) and 5(b), respectively, for different flock sizes.

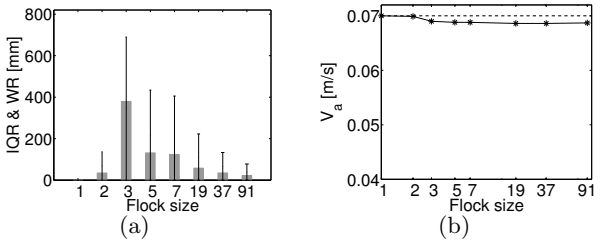

Figure 5: Proximal disturbance experiments. (a) Plot of IQR & WR for different flock sizes. (b) Plot of V_a with respect to flock size. The horizontal axis is in log scale. The dashed line indicates the value of the maximum forward speed $u_{max} = 0.07$ m/s.

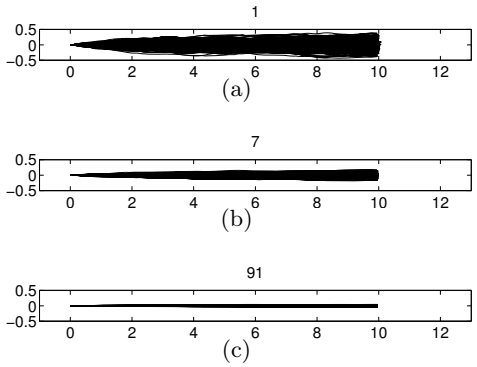

Figure 6: Noise in sensing the homing direction experiments. The paths followed by the flocks of (a) 1 robot, (b) 7 robots and (c) 91 robots for $\eta_S = 0.5$. The units of the axes are in meters. [0,0] is the starting point.

In Figure 5(a), IQR & WR follow a bell-shaped curve trend whose maximum is reached for 3-robot flock. Since the proximal control behavior is implicitly disabled for a "single robot flock", it follows always the same path resulting a zero IQR & WR. The average speed of single robot is at its maximum value as expected. For the increasing flock size the average speed decreases slightly.

6.2 Effect of noise in sensing the homing direction

The homing behavior aims to align the robots with the desired homing direction. Therefore, any error in sensing the homing direction would generate undesired deviations in the heading of the robots.

In order to investigate the effect of noise in sensing the homing direction, we vary η_S and conduct experiments with different sizes of flocks composed of identical robots. The proximal control is disabled in the experiments (whereas the noise in the IRSS is present) in order to discount its destructive effect on the alignment of the robots. The paths followed by the flocks for $\eta_S = 0.5$ are plotted in Figure 6. Figure 7 shows the resulting IQRs with respect to η_s for different flock sizes. Figure 8(a) plots the change in IQR &

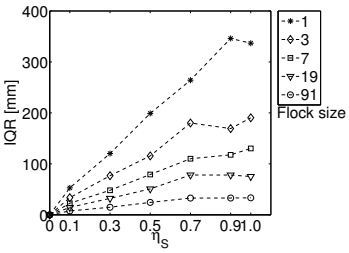

Figure 7: Noise in sensing the homing direction experiments. Plot of IQR with respect to η_S for different flock sizes.

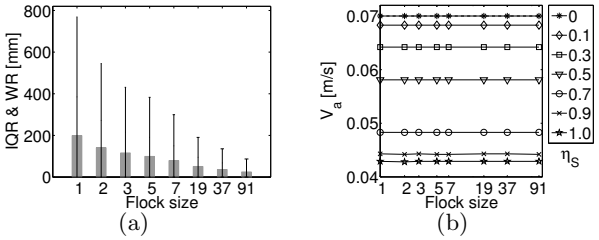

Figure 8: Noise in sensing the homing direction experiments. (a) Plot of IQR & WR for different flock sizes while $\eta_S = 0.5$. (b) Plot of V_a with respect to flock size for different values of η_S. The horizontal axis is in log scale. The dashed line indicates the value of the maximum forward speed $u_{max} = 0.07$ m/s.

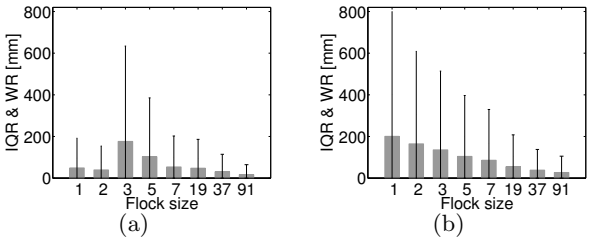

Figure 9: Individual difference experiments. IQR & WR plots for different flock sizes while (a) $\eta_S = 0.1$ and (a) $\eta_S = 0.5$.

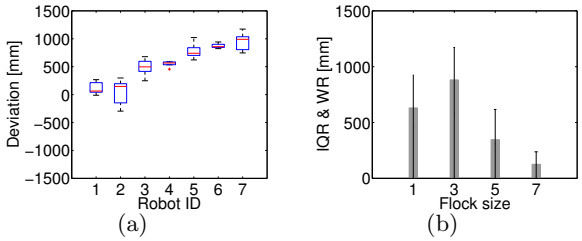

Figure 10: Kobot experiments. (a) Box-plot of the deviations at final positions. Note that due to a 6-degrees deviation of the magnetic field to the one side of the arena, deviation values are mostly positive. (b) Plot IQR & WR for different flock sizes.

WR for different flock sizes for $\eta_S = 0.5$. In Figure 8(b), the average speeds are given with respect to flock size for different values of η_S.

In Figure 6, the distribution of the paths gets narrower as the flock size increases. This is an indication of increase in the accuracy of the flocks with the flock size.

In Figure 7, IQRs are zero for all flock sizes when $\eta_S = 0$, which corresponds to the ideal case. When we increase the noise, IQR of small flocks increases rapidly while the increase in IQR of large flocks is slow. In a large flock, the individuals have more VHS neighbors and therefore averaging through heading alignment increases the robustness to the noise.

In Figure 8(a), both IQR & WR decrease as the flock size increases. The advantage of large flock size is evident in suppressing the noise in sensing the homing direction.

The average speeds in Figure 8(b) remain almost constant for the increasing flock size and decrease for the increasing noise. The decrease for the increasing noise is a result of large fluctuations in homing direction that cause the robots to turn more and hence get slower.

6.3 Effect of individual differences with noise in sensing the homing direction

If the individuals of a flock have different actuation characteristics, each of them is likely to follow a different path when they "migrate" alone. These different paths of different individuals create a large distribution in total. But what if they "migrate" together? Could there be an improvement in the accuracy? In the last set of the experiments, we search answers to these questions.

6.3.1 Simulations

In order to model the individual differences in simulations, we diversify 91 robots by adding an actuation noise to each robot as described in Section 5. Then, we randomly create 91 different flocks for each flock size from 91 diversified robots to be used in the simulations. The number of different flocks are kept constant for different flock sizes to guarantee that IQR & WR are calculated over the same number of experiments. For the flock size of 91, we obtain different flocks by changing the initial positions of the robots.

We conduct experiments by enabling the proximal control behavior and including noise in sensing the homing direction. The experiments are repeated 10 times for each flock. We plot IQR & WR in Figure 9(a) and 9(b) for different flock sizes and for $\eta_s = 0.1$ and $\eta_s = 0.5$, respectively.

In Figure 9(a), the effect of proximal disturbances is dominant and a similar trend as in Figure 5(a) is seen. For $\eta_s = 0.5$ in Figure 9(b), IQR & WR decrease as the flock size increases, which is an indication of improvement in the accuracy. This clearly shows that the tendencies of the individuals to migrate to different directions are suppressed with heading alignment and the effect of the suppression increases as the flock size gets larger resulting in an increase in the accuracy.

6.3.2 Experiments with Kobots

Kobots are inherently not identical. In order to evaluate individual differences, we conducted experiments with each of them. The resulting distributions of deviations at final position are given in Figure 10(a). Then, we conduct experiments with 1-, 3-, 5- and 7-robot flocks by selecting 7 different flocks for each flock size. Making only one experiment for a particular flock selected, we plot IQR & WR for each flock size in Figure 10(b). IQR & WR values for a particular flock size are calculated using the combined distribution of 7 experiments conducted for that flock size. Other than 3-robot flocks, there is a decreasing trend in IQR & WR indicating that the increase in the flock size increases the accuracy. The increase in IQR & WR of 3-robot flocks is caused by proximal disturbances.

7. CONCLUSION

In this paper, we study, from a constructivist view, how flocking affects the accuracy of robot swarms in "migrating" along a homing direction. We extend a self-organized flocking behavior to migrate a flock of robots from one place to another utilizing the magnetic field of the Earth. Our experiments conducted both with physical and simulated robots show that: (1) In order to suppress the effect of proximal disturbances, the flock size should be larger than a particular size. (2) Under the influence of sensor noise in sensing the homing direction, flocking increases the accuracy of migration. (3) When the individual characteristics differ from each other, the flocking improves the accuracy of the migration by suppressing the tendencies of the individuals to migrate to different directions. (4) Flocking does not have a large remedial effect on the average speed of the flocks.

8. ACKNOWLEDGMENTS

This work is funded by the TÜBİTAK research grant: 104E066. Fatih Gökçe is currently enrolled at the Faculty Development Program (ÖYP) in Middle East Technical University on behalf of Süleyman Demirel University.

9. REFERENCES

[1] R. C. Beason. Mechanisms of magnetic orientation in birds. *Integrative and Comparative Biology*, 45(3):565–573, June 2005.

[2] S. Benvenuti and N. Baldaccini. Pigeon orientation: A comparison between single birds and small flocks. *Ornis Scandinavica*, 16:45–48, 1985.

[3] G. Bergman and K. Donner. An analysis of the spring migration of the common scoter and the long-tailed duck in southern Finland. *Acta Zool. Fenn.*, 105:1–59, 1964.

[4] E. Codling, J. Pitchford, and S. Simpson. Group navigation and the "many-wrongs principle" in models of animal movement. *Ecology*, 88(7):1864–1870, 2007.

[5] G. Grégoire, H. Chaté, and Y. Tu. Moving and staying together without a leader. *Physica D*, (181):157–170, 2003.

[6] T. Guilford and J. Chappell. When pigeons home alone: Does flocking have a navigational function? *Biological Sciences*, 263(1367):153–156, 1996.

[7] A. Gutiérrez, A. Campo, F. C. Santos, C. Pinciroli, and M. Dorigo. Social odometry in populations of autonomous robots. In *Proc. of ANTS'08*, Lecture Notes in Computer Science, pages 371–378. Springer, 2008.

[8] W. Hamilton. Social aspects of bird orientation mechanisms. *Animal Orientation and Navigation*, pages 57–71, 1967.

[9] A. Hayes and P. Dormiani-Tabatabaei. Self-organized flocking with agent failure: Off-line optimization and demonstration with real robots. In *Proc. of the ICRA'02*, pages 3900–3905, 2002.

[10] W. Keeton. Comparative orientational and homing performances of single pigeons and small flocks. *Auk*, 87:797–799, 1970.

[11] I. Kelly and D. Keating. Flocking by the fusion of sonar and active infrared sensors on physical autonomous robots. In *Proceedings of The Third Int. Conf. on Mechatronics and Machine Vision in Practice*, volume 1, page 14, 1996.

[12] S. M. Perez, O. R. Taylor, and R. Jander. A sun compass in monarch butterflies. *Nature*, 387(6628):29, 1997.

[13] J. Rabøl and H. Noer. Spring migration in the skylark (Alauda arvensis) in Denmark. Influence of environmental factors on the flocksize and migratory direction. *Vogelwarte*, 27:50–65, 1973.

[14] S. A. Rommel, Jr., and J. D. Mccleave. Prediction of oceanic electric fields in relation to fish migration. *ICES Journal of Marine Science*, 35(1):27–31, 1973.

[15] G. Simon, P. Volgyesi, M. Maroti, and A. Ledeczi. Simulation-based optimization of communication protocols for large-scale wireless sensor networks. In *Proc. of the IEEE Aerospace Conference*, volume 3, pages 1339–1346, Big Sky, MT, March 2003.

[16] A. M. Simons. Many wrongs: The advantage of group navigation. *Trends in Ecology and Evolution*, 19(9):453–455, 2004.

[17] S. Tamm. Bird orientation: Single homing piegons compared with small flocks. *Behavioral Ecology and Sociobiology*, 7:319–322, 1980.

[18] A. E. Turgut, H. Çelikkanat, F. Gökçe, and E. Şahin. Self-organized flocking in mobile robot swarms. *Swarm Intelligence*, 2(2-3), 2008.

[19] A. E. Turgut, H. Çelikkanat, F. Gökçe, and E. Şahin. Self-organized flocking with a mobile robot swarm. In *Proc. of AAMAS'08*, pages 39–46, 2008.

[20] H. G. Wallraff. Social interrelations involved in migratory orientation of birds: Possible contribution of field studies. *Oikos*, 30:401–404, 1978.

[21] H. G. Wallraff. *Avian Navigation: Pigeon Homing as a Paradigm*. Springer-Verlag, Berlin, 2005.